Digital Discovery of Experimental Setups for Creating Highly-Entangled Quantum States

Bachelorarbeit aus der Physik

Author:	Jan Petermann Erwin Rommel Str 53 91058 Erlangen +49 1577 3923253 jan.petermann@fau.de 22704590
Submission:	5th November 2022

at Friedrich-Alexander-Universität Erlangen-Nürnberg
at the Max-Planck-Institut für die Physik des Lichts
Artificial Science Lab

Principal Supervisor:	Prof. Mario Krenn
Associate Supervisor:	Sören Arlt, Carlos Ruiz González

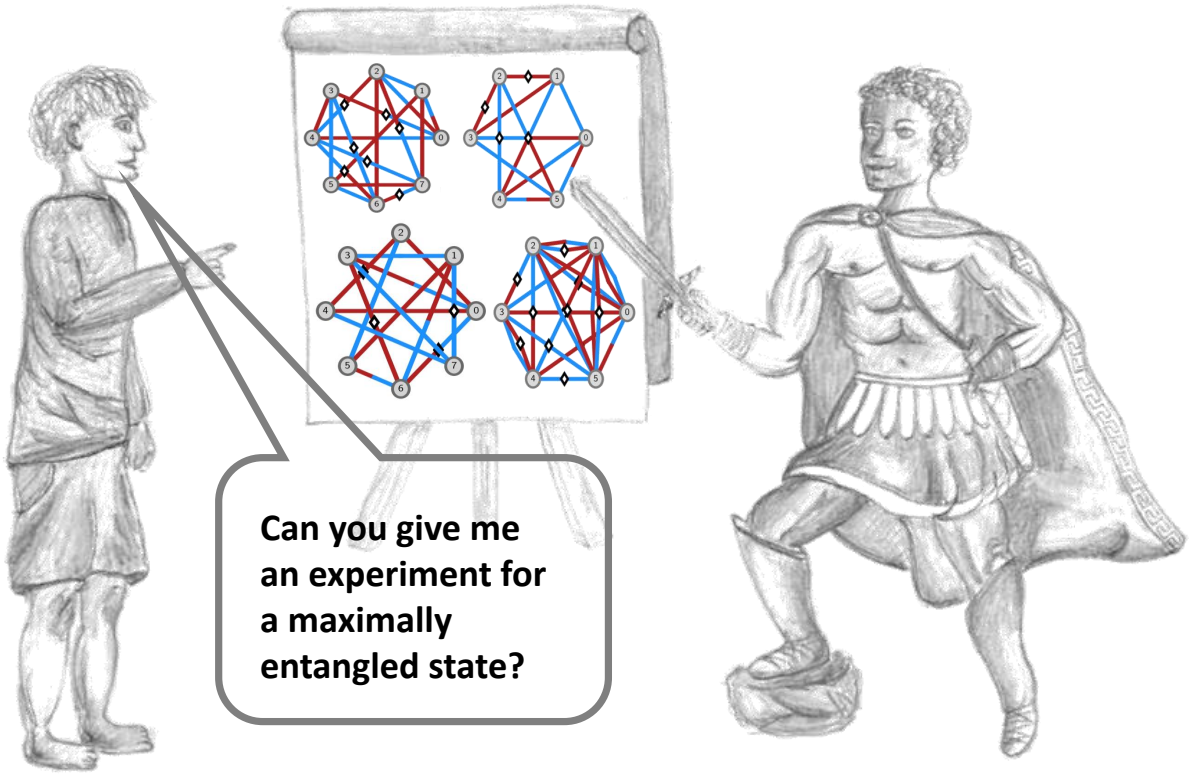
Can you give me an experiment for a maximally entangled state?

Abstract

In the following bachelor thesis, an existing artificial intelligence (AI) algorithm for the design of quantum optical experiments is extended. Instead of optimizing the count rate and state fidelity, an average over the purity of the subsystem served as the loss function. For a given system of N photons of different dimensionality d_i, one could thus specify the maximum possible entangled states for a given experimental setup. As a result, some experimental realizations of k uniform states and AMEs known from the literature could be found. This confirmed the functionality of the proposed algorithm and leaves open further investigations on higher dimensional and inhomogeneous systems.

Contents

Figures

Tables

Abbreviations

THESEUS AI algorithm with graph theory based approach for designing quantum experiments. (Krenn et al., 2021)

AME absolutely maximal entangled state

EPR Einstein-Podolsky-Rosen-Paradoxon

GHZ Greenberger–Horne–Zeilinger state, for definition see 2.1

HS Higuchi Sudbery-state (Higuchi & Sudbery, 2000)

PMs perfect matchings (see 2.5 for definition)

SQP sequential quadratic programming

1 Introduction

At least since the Nobel Prize in Physics [1] was awarded to Serge Haroche and David Wineland in 2012, public attention has turned to the field of quantum information(Union, 2021)(Union, 2019). The experimental methods developed in the process laid the foundation for many applications of quantum information theory. A well-known example is the quantum computer, which has the potential to revolutionize computing by making certain types of classically intractable problems solvable (Shor, 1997). Exciting examples can also be cited in quantum communication. Preventing information from being leaked to an illegitimate user is one of the most important issues today. Superdense coding (Bennett & Wiesner, 1992a), for example, enables secure communication and has already been implemented experimentally (Mattle et al., 1996). Bits are the logical states that classical information theory is based on. Much like that, quantum mechanical states form the basis of quantum information theory. Nevertheless, the creation of these states poses great challenges to scientists. The generation by photon source and linear components, for example phase shifters and beam splitters, is a frequently used approach. Even for experts it is sometimes not possible to derive a corresponding experimental setup. In recent years there have been some machine learning approaches that have tried to solve this problem, for example, the first algorithm capable of designing experiments - over ten of which have already been implemented, can be found in (Krenn et al., 2016). However, many of the approaches have drawbacks due to the complexity of the problem. One of the more successful graph theory based approaches called THESEUS was presented by (Krenn et al., 2021). THESEUS can be described as an automated design algorithm for quantum optics experimental setups. Thereby, THESEUS initialed the development from a non-transparent system towards an interpretable and explainable artificial intelligence, as the resulting graphs can be directly implemented by scientists in an experimental setup. Furthermore the graph representation allows for interpretation and generalization of the results. Previous efforts have been directed optimizing the fidelity of the created state with regard to a given target state. In the following, we will discuss how to extend the existing approach of THESEUS to search not only for states, but also for certain properties of states. To make it more concrete, the following question can be formulated. What is the maximally entangled state that can be produced with a given set of experimental constraints (linear optics, N photons of dimensionality d_i) and how does the corresponding experiment look like? Answering the first question requires an applicable measure for entanglement of multiparticle quantum systems.

[1] see https://www.nobelprize.org/prizes/physics/2012/press-release/ for more details

2 Theory

2.1 Quantum States

For a basic explanation of quantum information theory, it is best to start with the classical notion of the bit. From this, a bridge can be built to quantum information theory. In digital systems, a bit can take either zero or one. An experimental realization is very easy to achieve here. For example, with different voltage levels, positive voltage corresponds to one and negtive voltage to zero. The counterpart to the bit in quantum information theory is the so-called qubit. A qubit is a quantum system with two states, for example a physical realization would be the spin of an electron, which is either directed upwards or downwards in a given reference frame, or one uses a photon, which has a vertical or a horizontal polarization. Mathematically one can make use of Hilbert space properties with basis $|0\rangle$ and $|1\rangle$, then a qubit can be written as (Schumacher, 1995)

Definition 2.1.1 (Qubit)**.**

$$|\Phi\rangle = \alpha\,|0\rangle + \beta\,|1\rangle \qquad |\alpha|^2 + |\beta|^2 = 1, \tag{2.1}$$

where $\alpha, \beta \in \mathcal{C}$. From this definition the difference between classical and quantum systems can already be guessed. While a bit is always in one of the two states, a qubit can be in a superposition of both states. It is also possible to describe systems containing n qubits. Here, the total Hilbert space $\mathcal{H} = \mathcal{H}_1 \otimes \cdots \otimes \mathcal{H}_n$ is the tensor product of the single Hilbert spaces for each qubit. One example is the generalized GHZ state, studied by (Greenberger et al., 2007)

$$|\mathrm{GHZ}\rangle = \frac{1}{\sqrt{2}}(|0\rangle \otimes \cdots \otimes |0\rangle + |1\rangle \otimes \cdots \otimes |1\rangle\,.$$

For a system of two qubits, there are four basis states. With the usual notation, the Bell states e_i are among the most used basis states in quantum information science.

$$\begin{aligned}
|e_1\rangle &= \frac{1}{\sqrt{2}}(|0_1 0_2\rangle + |1_1 1_2\rangle) \\
|e_2\rangle &= \frac{1}{\sqrt{2}}(|0_1 0_2\rangle - |1_1 1_2\rangle) \\
|e_3\rangle &= \frac{1}{\sqrt{2}}(|0_1 1_2\rangle + |1_1 0_2\rangle) \\
|e_4\rangle &= \frac{1}{\sqrt{2}}(|0_1 1_2\rangle - |1_1 0_2\rangle)
\end{aligned} \tag{2.2}$$

Consider a quantum mechanical measurement with operator $\Omega_1 = \Omega \otimes I_2$ acting on the first qubit and $\Omega\,|0\rangle = \lambda\,|0\rangle$. Where $\lambda \in \mathcal{R}$ is the associated eigenvalue and I_2 is the

identity in the Hilbert space of the second qubit. If one gets the result λ after doing a measurement Ω_1 on state e_1 the state collapses to $|00\rangle$. That means instantaneously the state of the second qubit is fixed independently of the spatial instance of the two qubits. This is the origin of the EPR paradox, which Einstein is said to have already called „spukhafte Fernwirkung“ („spooky action at a distance“) (Kiefer, 2015). In the next chapter we will have a closer look at this effect.

2.2 Entanglement

A long-running discussion in the thirties was Einstein's concept of "local realism"(Einstein et al., 1935). One calls a theory *local*, if an influence between two space separated particles can propagate only with speed of light. One speaks of a *realistic* theory if one can predict the physical system with certainty without disturbing it. Einstein noticed that quantum mechanics could not be assigned both properties and concluded that it was incomplete. Later, John Stewart Bell was able to show that, if one follows this concept, in certain experiments on pairs of particles the results of measurement should always satisfy an inequality. However, quantum theory predicts the violation of the inequality in certain cases for entangled particles. That violation was demonstrated by many experiments so far (Weihs et al., 1998) (Aspect, 1999) (Giustina et al., 2015). Entanglement is thus a key feature of quantum mechanics and excludes the simultaneous existence of the two principles of *locality* and *realism* observation of quantum physical systems. While classical correlation exists also in quantum mechanic (mixed states), entanglement has no analogue in classical theory. At least since the discovery of possible practical applications such as quantum teleportation (Raissi et al., 2018), quantum error correcting codes (Raissi et al., 2018) and superdense coding (Bennett & Wiesner, 1992b), it has become a major component of current research. However, the single characterization of entanglement for arbitrary multipartite states is challenging. In recent years, a class of so called k-uniform states has attracted attention. One calls a n-partite state k-uniform if every density matrix reduced to reduced to parties of size k is maximally mixed (Goyeneche & Życzkowski, 2014). For the special case of a $\lfloor \frac{N}{2} \rfloor$-uniform state one calls those absolutely maximally entangled (AME). AME states have application in threshold quantum secret sharing schemes (QSS) and can be used for open-destination teleportation protocols (Helwig, 2013).

Definition 2.2.1 (Entangled Pure State)**.** Consider a pure state $\Psi_{AB} \in \mathcal{H}_A \otimes \mathcal{H}_B$. Then we call a state entangled if and only if it cannot be factored into the direct product of arbitrary pure states $\Psi_A \in \mathcal{H}_A$ and $\Psi_B \in \mathcal{H}_B$. That means $\Psi_{AB} \neq \Psi_A \otimes \Psi_B$ for any choice of Ψ_A and Ψ_B (Guedes et al., 2016).

It has already been mentioned that for an entangled system, certain properties of system A are correlated with system B even if the systems are spatially separated from each other. To make it clearer we can have a look at an example. The state

$$|\Psi_1\rangle = \frac{1}{2}\left(|00\rangle - |01\rangle - |10\rangle + |11\rangle\right)$$

is not entangled because it can simply be expressed as a product state

$$|-\rangle_{\mathsf{A}} \otimes |-\rangle_{\mathsf{B}} = \left[\frac{1}{\sqrt{2}}(|0\rangle - |1\rangle)\right] \otimes \left[\frac{1}{\sqrt{2}}(|0\rangle - |1\rangle)\right] = |\Psi_1\rangle \ .$$

Looking at the first Bell state state defined in 2.2, one can see that it can not be expressed as a tensor product between two Qubits A,B.

$$|e_1\rangle \stackrel{!}{=} (\alpha\,|0\rangle_A + \beta\,|1\rangle_A) \otimes (\gamma\,|0\rangle_B + \delta\,|1\rangle_B) =$$
$$\alpha\gamma\,|0_A 0_B\rangle + \alpha\delta\,|0_A 1_B\rangle + \beta\gamma\,|1_A 0_B\rangle + \beta\delta\,|1_A 1_B\rangle$$

The two equations $\alpha\gamma = \beta\delta = \frac{1}{\sqrt{2}}$ and $\alpha\delta = \beta\gamma = 0$ contradict one another. Thus the state can not be written in a seperable form. That means the e_1 state is entangled because it can not be split into two separate qubit pure states. One can now extend this formalism to higher dimensions and multi-particle-systems. Consider a n-particle pure quantum system.

Definition 2.2.2. Let $A|B$ be a given bipartition for the system satisfying $\mathcal{H} = \mathcal{H}_A \otimes \mathcal{H}_B$. If a state $|\Psi\rangle \in \mathcal{H}$ can be written in a form

$$|\Psi\rangle = |\phi\rangle_A \otimes |\xi\rangle_B \,,$$

the system is separable across the bipartition $A|B$. If this is not possible, the two subsystems are entangled.

To quantify entanglement properties of a given state, we need a function that maps a given state density matrix to a scalar with the following properties.

Definition 2.2.3 (entanglement monotone)**.** A function $E(\rho)$ that maps density matrices ρ into positive real numbers $E(\rho) \in \mathbb{R}^+$ is called entanglement monotone when it satisfies the following properties (Plbnio & Virmani, 2007):

1. $E(\rho) = 0 \Leftrightarrow$ the corresponding state is separable.
2. E does not increase on average under local operations and classical communication. That means on average $E(\Lambda\text{LOCC}[\rho]) \leq E(\rho)$.

A stricter definition is an entanglement measure. It introduces the additional requirement that for a pure state $\langle\Psi|\Psi\rangle$ the measure reduces to the entropy of entanglement $(S \circ \mathrm{Tr}_B)(\langle\Psi|\Psi\rangle)$ (Plbnio & Virmani, 2007). In contrast to property (2), it does not increase under deterministic LOCC transformations. In the literature these terms are often used synonymously. In addition, further properties like additivity and convexity for entanglement measures can be defined which are not important for further understanding. Thereby the question can be specified, if one wants to measure the entanglement only between two given subsystems or if one wants to consider a global measure. Here it is important to distinguish between a simple bipartite treatment or a whole sum over all bipartitions as the following definitions explain.

Definition 2.2.4 (bipartition and partial Trace)**.** For a given system with n particles of dimension d we can define the partial trace with respect to a given bipartition $(A|\bar{A}$, made up of n_A and $n_{\bar{A}}$ particles as follows

$$\mathsf{Tr}_B \rho_{AB} = \mathsf{Tr}_B \left(\sum_{i,j,k,l} c_{i,j,k,l} \left|a_i\right\rangle \left\langle a_j\right| \otimes \left|b_l\right\rangle \left\langle b_k\right| \right) = \sum_{i,j,k,l} c_{i,j,k,l} \left|a_i\right\rangle \left\langle a_j\right| \left\langle b_l|b_l\right\rangle \tag{2.3}$$

, where with basis $\{\langle a_i|\}$ and $\{\langle b_i|\}$ for $\mathcal{H}_A$ and $\mathcal{H}_B$ respectively.

For a better understanding, it might be helpful to keep track of the dimensions. The total dimension of the entire Hilbert space is $D_{\text{total}} = D_A \cdot D_B$, where one can calculate $D_A = d^{n_A}$. Furthermore, it is important to notice that one can split a given state in a lot of different ways. For example, we can have a look at four Qubits A, B, C, D. For this given system one finds 7 different bipartitions $\{(A|BCD), (B|ACD), C|ABD), (D|ABC),$ $(AB|CD), (AC|BD), (AD|CD)\}$. Here, it can already bee seen that there are different types of bipartitions. Namely those which are grouped in pairs of two particles and those where a single particle is separated from the remaining ones. This leads us to the next definition.

Definition 2.2.5 (k - bipartition)**.** We call a bipartition $(A|\bar{A})$ a k - bipartition when A has cardinality of k. Without loss of generality one choose the set A such that $|A| \leq |\bar{A}|$ holds.

In our previous example one would have four 1-bipartitions and three 2-bipartitions. With the introduction of the concept of bipartition, it is now possible to define entanglement measurements that can be defined for any quantum state and also take into account a multipartite entanglement. For a given state and a given bipartition there exists many entanglement measurements, e.g. the entropy and the concurrence. In the following we will have a look how one can define the different entanglement measures and how one can extend it for all possible bipartitions.

2.3 Concurrence and Purity

An entanglement monotone called concurrence was introduced by (Hill & Wootters, 1997). Given a pure state $|\Psi\rangle = \sum_i \alpha_i |e_i\rangle$ written in the Bell basis e_i (2.2). The concurrence reads

$$C(\Psi) = |\langle\Psi^*|\Psi\rangle| = |\sum_i \alpha_i|^2. \tag{2.4}$$

It characterizes the total overlap of the state $|\Psi\rangle$ with these four maximally entangled bell states. (Rungta et al., 2001) generalized this definition for high dimensions to the so called I-concurrence.

Definition 2.3.1 (I-concurrence)**.** For a pure state $|\Psi\rangle$ the concurrence reads

$$C(\Psi) = \sqrt{2 \cdot (1 - \operatorname{Tr} \rho_{\text{red}}^2)}, \tag{2.5}$$

where ρ_Ψ is the density matrix $|\Psi\rangle\langle\Psi|$ from Ψ and $\rho_{\text{red}} = \text{Tr}_B \rho_\Psi$ the reduced density matrix.

The concurrence has a clear geometric interpretation. Consider a two qubit system. One can write a pure state as

$$\begin{aligned} |\phi\rangle &= \alpha |0_A 0_B\rangle + \beta |0_A 1_B\rangle + \gamma |1_A 0_B\rangle + \delta |1_A 1_B\rangle \\ &= |0_A\rangle \underbrace{(\alpha |0_B\rangle + \beta |1_B\rangle)}_{\langle 0_A|\phi\rangle} + |1_A\rangle \underbrace{(\gamma |0_B\rangle + \delta |1_B\rangle)}_{\langle 1_A|\psi\rangle}. \end{aligned}$$

Regarding the definition of separability for a pure state (2.2), one can separate the state $|\phi\rangle$ when the two vectors $\langle 0_A|\phi\rangle$ and $\langle 1_A|\phi\rangle$ in Hilbert space $\mathcal{H}_B$ are parallel. This is equivalent to

$$\alpha\delta - \gamma\beta = 0$$

(Bhaskara & Panigrahi, 2017) showed that one can write the requirement $|\alpha\delta - \gamma\beta| = || \langle 0_A|\phi\rangle \wedge \langle 1_A|\phi\rangle || = 0$ .The wedge product $\wedge$ is an generalization of the cross product to higher dimensions. That means $|| \langle 0_A|\phi\rangle \wedge \langle 1_A|\phi\rangle ||$ represents the area of the parallelotope spanned by the two vecors in the Hilbert space $\mathcal{H}_B$. For maximal entanglement the two vectors should be perpendicular to each other. That means the resulting parallelotope is a square. From the normalization constraints the side length is equal to $\frac{1}{\sqrt{2}}$. Figure 1 shows an illustration of the two vectors in the Hilbert space $\mathbb{H}_B$ for different states. One can see that the Bell state e_1 and $|\Psi\rangle$ are maximally entangled. The state $|\Phi\rangle$, on the other hand, is not, since the vectors do not form a square. They are closer to being parallel. (Bhaskara & Panigrahi, 2017) generalized this concept also to higher dimensions. Now, one can see that maximizing the concurrence of a state is equivalent to minimizing the purity of the reduced density matrix purity $= \operatorname{Tr} \rho^2$.

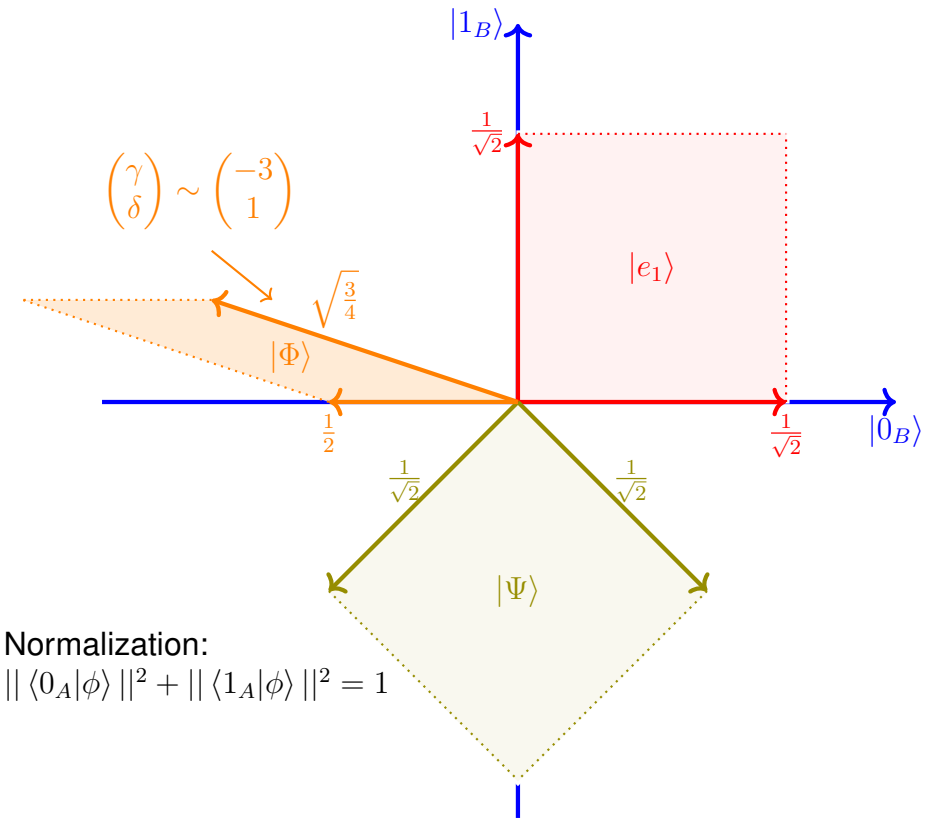

Figure 1 Geometric interpretation of the concurrence. The two vectors for each state symbolize $\langle 0_A|\phi\rangle$ and $\langle 1_A|\phi\rangle$. For the $|e_1\rangle$ one directly sees that $\beta = 0$ and $\gamma = 0$ resulting in $|00\rangle + |11\rangle$. For $|\Psi\rangle$ one gets $\alpha = 1$ and $\beta = -1$ (vector right bottom) and $\gamma = \delta = -1$. That results in $|\Psi\rangle = |00\rangle - |01\rangle - |10\rangle - |11\rangle$. The same procedure leads to $|\Phi\rangle = -|00\rangle - 3\,|10\rangle + 1 \cdot |11\rangle$

2.4 AME and k-uniform States

Definition 2.4.1. A state $|\Psi\rangle \in \mathcal{H}_1 \otimes ... \otimes \mathcal{H}_N$ is called k-uniform when it satisfies

$$\forall\,(B \subset I : |B| = k): \quad \rho_B = \mathrm{Tr}_{B^c}\,|\Psi\rangle\,\langle\Psi| = \frac{1}{d^k}\mathbb{I}_B, \tag{2.6}$$

where $I = \{1, ..., N\}$ and the partical trace Tr_{B^c} is acting on the complement $B^c = I \setminus B$. $\mathbb{I}_B$ is the identity matrix in $\mathcal{H}_B = \bigotimes_{b\in B} \mathcal{H}_b$. The bipartition is then $\{B, B \setminus I\}$.

Resulting in a identity matrix after doing the partial trace the state is maximally entangled according to the given bipartion. Then the resulting vectors $\langle 0_A|\phi\rangle$ and $\langle 1_A|\phi\rangle$ span a high dimensional square comparing to figure 1. For N qudit systems of d levels the generalized GHZ state $|\mathrm{GHZ}\rangle = \frac{1}{\sqrt{d}}\sum_{i=0}^{d-1} |i\rangle^{\otimes N}$ is for example an one uniform state. It is known that there exists no two-uniform state for a system of four qubits (Gour & Wallach, 2010) but one can search for states being one uniform and whose average purity of the reduced states for the bipartitions with $|B| = 2$ appears to be maximal. Those

states are called maximally multi-qubit entangled state (MMES) (Zha et al., 2013). For 4-qubits there exist many MMES. For instance, the HS state defined by (Higuchi & Sudbery, 2000)

$$|\mathrm{HS}\rangle = |0011\rangle + |1100\rangle + \omega\left(|0101\rangle + |1010\rangle\right) + \omega^2\left(|1001\rangle + |0110\rangle\right) \quad \omega = e^{\frac{2}{3}i\pi}$$

When equation 2.6 is satisfied for $k = \lfloor \frac{N}{2} \rfloor$ it can be proven that the state is also $\bar{k}$-uniform with $\bar{k} <= k$ (Scott, 2004). That is important to notice because when one optimizes for an k uniform state there is no need to computing the reduced density matrices for the bipartitions with length $\bar{k} <= k$. For an AME we can note the following characteristics.

Definition 2.4.2. Absolutely maximally entangled states can be identified by the following equivalent and sufficient conditions (Helwig, 2013).

- $|\Psi\rangle$ is maximally entangled for any possible bipartition. That means that all reduced density matrices ρ_B for all possible subsets $B \subset I : |B| \leq \lfloor \frac{N}{2} \rfloor$ are totally mixed.
- The von Neumann entropy and concurrence of every subset are maximal.

As the requirements for such states are high, as already mentioned, there is no AME for every system. Table 1 shows a section for systems of N particles of dimension D. This indicates whether an AME exists for the respective system or if it is uncertain or whether it could be proved that it cannot exist. If the respective AME does not exist, the maximum possible k-uniform state is given.

D,N	2	3	4	5	6	7	8	9	10
2	1	1	2	2	3	3	4 (3)	4 (3)	5 (3)
3	1	1	2	2	3	3	4 (3)	4	5
4	1	1	2	2	3	3	4	4	5
5	1	1	2	2	3	3	4	4	5

Table 1 Green: AME exists, red: AME does not exist, yellow: unknown, number is maximal k-uniform and brackets: maximal k if AME does not exist (Shi et al., 2020) (Goyeneche & Zyczkowski, 2014).

2.5 Theseus

In contrast to classical systems the design of experimental setups for a given quantum system is challenging. The reason for this is the exponential rising size of the

Hilbert spaces for bigger system and corresponding increasing combinatorial calculations makes it hard for a scientist to design a proper experimental setup. In (Krenn et al., 2021) an approach based on graph theory called THESEUS, an explainable AI algorithm is given. For a given graph $G(E,V)$ with a set of bi-colored edges $E = \{e_1^2, ..., e_n^{n+1}\}$ and vertices $V = \{v_1, ..., v_n\}$, where e_i^j is the edge between the vertex v_i and v_j. To translate the Graph G one defines the following. The vertices correspond to given photon paths. An edge e_i^j between vertex v_i and v_j represent a probabilistic photon pair creation in path v_i and v_j. The two colors of the edges symbolizes the mode of the photon entering the respective path. Moreover, the weight ω of the edge correlates to the amplitude. One can define a weight function to map the graph to state. This weight function contains a term of two creation operators for each edge of the graph, representing the pair creation associated with it. By applying $\Psi(\omega)$ to the vacuum state

$$|\phi\rangle = \Psi(\omega)\,|Vac\rangle \tag{2.7}$$

one gets the resulting state $|\phi\rangle$. Here one can already notice that the resulting state depends on the weights ω. That means one can use optimization techniques such as gradient descent methods to optimize the weights. A common technique presented in (Krenn et al., 2021) is to start with a full graph containing all possible edges. First, one optimizes the weights and deletes those being smaller than a given threshold. Afterwards, a topological optimization is performed. The weights in ascending order are deleted and the resulting graph is kept if the loss function does not fall below a certain value. That result in a small graph a scientist can interpret and translate to different types of quantum optical implementations. In the following we only focus on linear terms. Higher order terms resulting from single photon non-lineareties will be ignored. A prominent technique is to condition the photons by simultaneous detection in each path.

Figure 4 shows an example graph with a corresponding experimental setup for a state that reads $|\phi\rangle = \frac{1}{\sqrt{2}}(|1_a 2_b 0_c 0_d\rangle + |1_a 1_b 0_c 0_d\rangle)$. Where the subscripts stand for a photon in the given path with mode 0,1 or 2. The given graph has two perfect matchings pictured in 4. A perfect matching is a subgraph G_{sub} covering every vertex of the graph $G(E,V)$ exactly once. To translate a graph into a state, one can proceed as follows, first, all perfect matching must be found. Each perfect matching can be assigned a ket (according to the colors assigned to each vertex. All perfect matchings for a ket are added together. The resulting state is the sum of the weighted kets with the corresponding normalization. Comparing 4 IV and the assumption of simultaneous detection of a photon in each of the detectors $A - D$ there are two possible options for a four photon constellation. The first is that the photons come from $\omega_{A,B}^{1,2}$ and $\omega_{C,D}^{0,0}$ (first perfect matching) or from $\omega_{A,C}^{1,0}$ and $\omega_{B,D}^{1,0}$ (second perfect matching). The resulting state is the sum

of both possibilities weighted with the amplitudes for each state that results from the corresponding perfect matching. Further experimental setups can be found in Figure to generate the state explained in Figure 4.

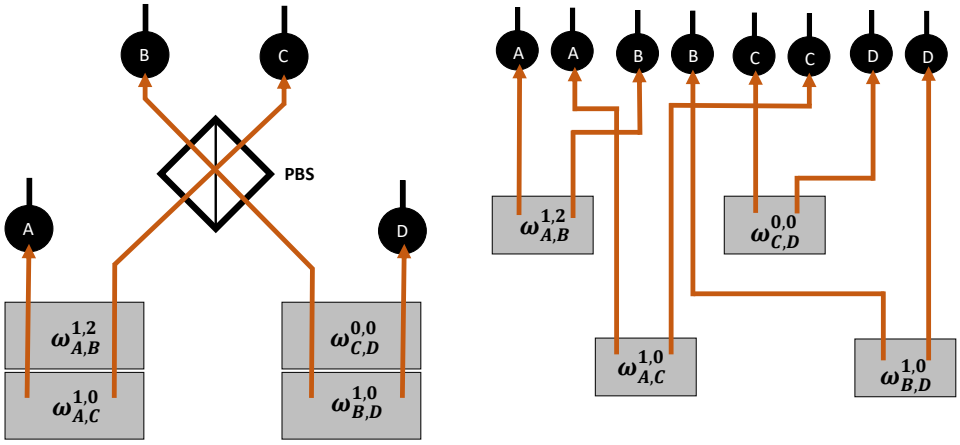

Figure 2 The left standard bulk optics is used, where PBS stands for polarizing beam splitter. The right shows a setup called integrated photonics (Wang et al., 2019). Same notation is used as in Figure 4

Epsilon Solution

Some optimizations result in what we call an epsilon solution. That are solutions for which the target state fidelity approaches one only as the pump rate proportional to the scaling of the weights is decreased towards zero. An example is shown in figure 3. Here, THESEUS found a solution for the three-dimensional six-photonic GHZ state $|000000\rangle + |111111\rangle + |222222\rangle$. Three PMs create each of the three kets. However, there is another PMs which creates an additional ket that reads $|100122\rangle$. To minimize the contribution of this cross term in comparison to the target terms, each edge of the additional perfect matching is assigned a weight ϵ. For $\epsilon \to 0$ this ket goes faster to zero ($\propto \epsilon^3$) than the required kets ($\propto \epsilon$).

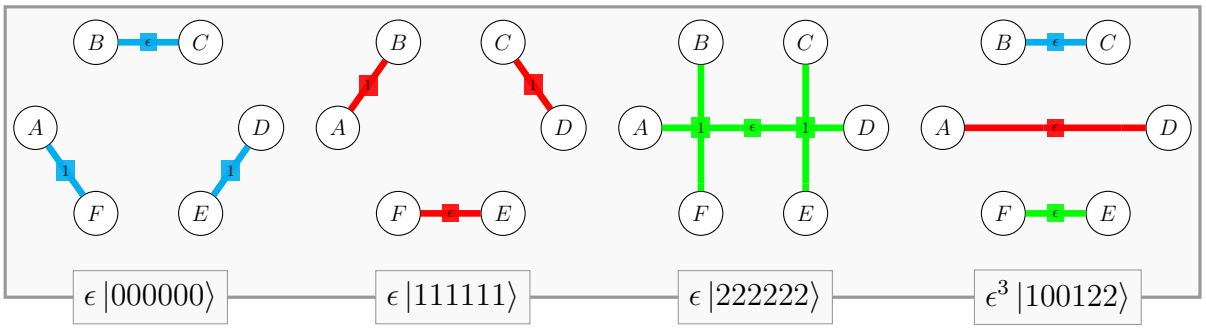

Figure 3 All PMs of the epsilon solution of the three-dimensional six-photonic GHZ state (Krenn et al., 2021).

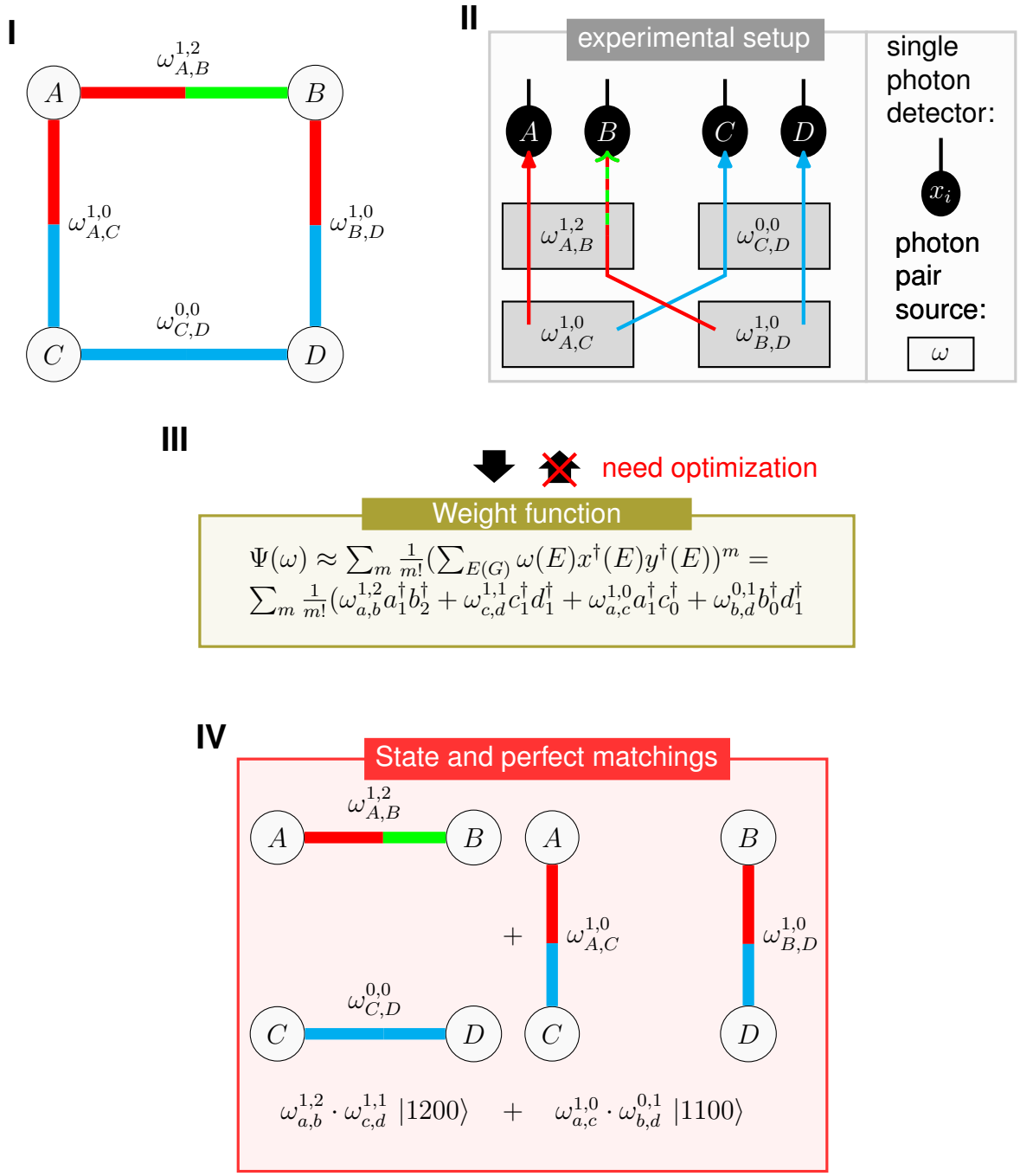

Figure 4 I shows an example graph with four edges and 4 vertices. II shows an example experimental realization of the graph. Thereby all gray squares represents probabilistic pair sources generating photon pairs. The colored lines mark the photon path with their corresponding mode. The black circles stand for single photon detectors. III shows the weight function $\Psi(\omega)$ applied on the given graph in I. For a given graph its translation into the corresponding state is straightforward to calculate, but the inverse is not. IV shows all PMs of the graph and the resulting state for each perfect matching.

2.6 Loss function and Optimization Algorithm

We have seen that we can transform a graph $G(E, V)$ into a state depending on its weights ω. If we want to generate a given state $|\Psi\rangle$, we can define the fidelity of the state $|\Psi\rangle$ and the state $|\Psi_{\mathsf{G}}\rangle$ generated by the graph as a loss function $\mathcal{L} = \langle|\Psi\rangle|\Psi_{\mathsf{G}}\rangle$. This approach was also followed in (Krenn et al., 2021). Since it is not clear from the beginning, what is the most highly entangled state to achieve with the given resources, i.e. number of photon sources, it makes sense to optimize according to a property of a state. In this case we will choose a loss function that can find different k uniform states. One can now choose between different loss-functions $\mathcal{L}_k$. In order to optimize for creating the maximal entanglement possible with given resources, we choose an entanglement monotone $\pi(\rho)$ such as the entropy or the concurrence as the loss function. For computational reasons it is suitable to choose the purity $\pi(\rho) = \mathrm{Tr}\,\rho^2$ in white to (Zha et al., 2013) (Scott, 2004).

Definition 2.6.1 (loss function $\mathcal{L}_k$)**.** We define the loss as the sum over a bipartite entanglement for a given set M of bipartitions

$$\mathcal{L}_k(G) = \mathcal{L}_k(|\Psi\rangle) = \sum_{m \in M_k} \pi(\rho_m), \tag{2.8}$$

where $\rho_m = \mathsf{Tr}_{m^c}|\Psi\rangle\langle\Psi|$ is the reduced density matrix for a given bipartition b. $\mathcal{L}_k(G) = \mathcal{L}_k(|\Psi\rangle)$ means that Ψ is the resulting state of the graph G.

If one wants to optimize to obtain a k - uniform state one can choose M such that it contains all bipartitions of length k. An initial graph G_{start} with weights $\omega \in \mathbb{R}^{|G|}, \mathbb{C}^{|G|}$ is constructed containing all possible edges for the given system. Afterwards, the graph is optimized by solving

$$\min_{\omega \in \mathbb{R}^{|G|}, \mathbb{C}^{|G|}} \mathcal{L}_k(G(\omega)). \tag{2.9}$$

The edge with the smallest weight with respect to the magnitude is deleted. Then, the difference between the loss function $\mathcal{L}_k(G)$ and the loss $\mathcal{L}_k(G_{reduced})$ is compared to a threshold. If it holds a certain threshold one updates the graph $G = G_{reduced}$. If this was not successful the graph is optimized again with random weights. This is done a maximum of tries_per_edge times. Those steps are continued as long as the amount of edges of the graph G does not fall below a certain value min_edges or all edges have been tried. The resulting graph has fewer edges than the initial graph G_{start}, but has almost the same loss if the threshold is chosen appropriately. The algorithm is summarized in 0. Additionally, one can add the variance of the resulting values $\pi(\rho_m)$ to the loss function weighted with a factor var_fac. That makes sure that the entanglement is distributed equally over all bipartions.

Algorithm 1 The topological algorithm for optimizing highly entangled state.

Require: Full starting Graph $G_{start}(\omega)$ with all possible edges for given dimension
initialization $n_{th} = 0$, $G = G_{start}(\omega)$,
while amount of edges `min_edges` < $|G|$ and $n_{th} <= |G|$ **do**
remove edge $\omega_{n_{th}}$ with n_{th} smallest weight from G resulting in $G_{reduced}$,
for $try \in \{0, ..., \texttt{tries\_per\_edge}\}$ **do**
if $try \neq 0$ **then**
$\omega = \min_{\omega \in \mathbb{R}^{|G|}, \mathbb{C}^{|G|}} \mathcal{L}_k(G_{reduced}(\omega_{red}))$,
else
$\omega = \omega$, ▷ keep weights from previous graph
if $\mathcal{L}_k(G_{reduced}) - \mathcal{L}_k(G)$ < `threshold` **then**
set $G = G_{reduced}$,
`success = true`,
break ,
if `success is false` **then**
keep G and set $n_{th} += 1$ for trying next edge ,

Consider a system of four qubits. The maximal k one can choose is $k = 2$. Assume that $|\Psi\rangle = |0011\rangle + |1100\rangle + |1010\rangle + |0101\rangle$ and for the loss function in equation 2.8 we choose $\pi(\rho) = \mathrm{Tr}[\rho^2]$. The reduced density matrices for tracing out the last three particles reads

$$\mathrm{Tr}_A\rho = \rho_A = \frac{1}{4}|0\rangle\langle 0| + \frac{1}{4}|1\rangle\langle 1| + \frac{1}{4}|0\rangle\langle 0| + \frac{1}{4}|1\rangle\langle 1| = \frac{1}{2}I_2. \tag{2.10}$$

In the same way, one results in the identity for the remaining three splits into one particle and the remaining ones. For $k = 1$ the loss function is minimized because it easy to see that

$$\mathcal{L}_{k=1}(|\Psi\rangle) = \sum_{m\in\{A,B,C,D\}} \mathrm{Tr}(\underbrace{\rho_m}_{\forall m = \frac{1}{2}I_2})^2 = 2,$$

where $|\Psi\rangle$ is 1-uniform but for $k = 2$ for the splits $\{AB, CD\}$ and $\{AC, BD\}$ the reduced density matrix also leads to the identity $\frac{1}{4}I_4$ but for the split $\{AD, BC\}$ the reduced density matrix reads

$$\rho_{AD} = \frac{1}{2}(|01\rangle\langle 01| + |10\rangle\langle 10| + |01\rangle\langle 10| + |10\rangle\langle 01|). \tag{2.11}$$

If you insert this into the loss function you get

$$\mathcal{L}_{k=2}(|\Psi\rangle) = \underbrace{2\cdot\mathrm{Tr}\left[\left(\frac{1}{4}\cdot I_4\right)^2\right]}_{\text{For } \{AB,CD\} \text{ and } \{AC,BD\}} + \underbrace{\mathrm{Tr}\left[\left(\frac{1}{2}\right)^2 \begin{pmatrix} 0&0&0&0\\ 0&1&1&0\\ 0&1&1&0\\ 0&0&0&0 \end{pmatrix}^2\right]}_{\text{For } \{AD,BC\}} = \frac{3}{2} > \frac{3}{4} = \mathcal{L}^{\min}_{k=2}.$$

One can see that $|\Psi\rangle$ is not 2 - uniform because the reduced density matrix for the bipartition $\{1, 4\}$ is not the identity.

2.6.1 Optimizer

For the optimization problem defined in 2.9 an iterative method for constrained nonlinear optimization is used called Sequential quadratic programming (SQP). In our case the problem reads

$$\min_{\omega \in \mathbb{R}^{|G|}, \mathbb{C}^{|G|}} \mathcal{L}\left(G(\omega)\right) \quad \text{s.t.} \quad g(\omega) = |\omega| - 1 \leq 0 \tag{2.12}$$

One can Taylor expand $\mathcal{L}$ up to quadratic order with Hessian $H_{\mathcal{L}}$ and g linear. Then, the SQP solves the problem iteratively. Starting from ω^k one solves (Bartholomew–Biggs, 2008)

$$\begin{aligned} \widetilde{\mathcal{L}}(\omega^k + d) := \nabla\mathcal{L}(\omega^k)^T d + d^T H_{\mathcal{L}}(\omega^k) d \to \min_{d \in \mathbb{R}^n, \mathbb{C}^n}, \\ \text{s.t.} \\ \tilde{g}(\omega^k + d) := g(\omega^k) + \nabla g(\omega^k) d \leq 0 \end{aligned}$$

and the update step is done with

$$\omega^{k+1} = \omega^k + d^k.$$

Thus, for the SQP a linear quadratic optimization problem has to be solved in each iteration. This is done with conventional methods, for example on the reduction $Ad = b$. In our case, it is straightforward to show that the quation system is given by

$$A = \begin{bmatrix} H_{\mathcal{L}}(\omega) + H_{\mathcal{L}}^T(\omega) & \nabla g^T(\omega) \\ \nabla g(\omega) & 0 \end{bmatrix} \quad \text{and} \quad b = \begin{bmatrix} -\nabla\mathcal{L}(\omega) \\ -g(\omega) \end{bmatrix}.$$

2.6.2 Source Code

Figure 5 shows a schematic overview over the library THESEUS. First, the config file is used to setup the initial graph. The initial graph is input for the class `topological_opti`. The class method `pre_optimize_start_graph` pre-optimizes the graph `pre_opt` times. After passing the resulting graph to `topologicalOptimization` a while loop is performed until the `termination_condition` is fulfilled. Within the while loop `optimize_one_edge` deletes an edge and performs an optimization. When `check` is successful the reduced graph is kept. Otherwise, we optimize the current edge again `tries_per_edge` times. In the end, the graph is saved using the class `saver`. For an analysis of the results the class `analyzer` is available with two main functions.

`info_statex` generates an overview plot of different information and the function `all_perfect_matchings_to_pdf` saves a pdf containing all graphs of the possible perfect matchings. The explained code is available in GitHub[2] as part of a larger python library implementing digital discovery of experimental setups for a range of quantum optical experiments.

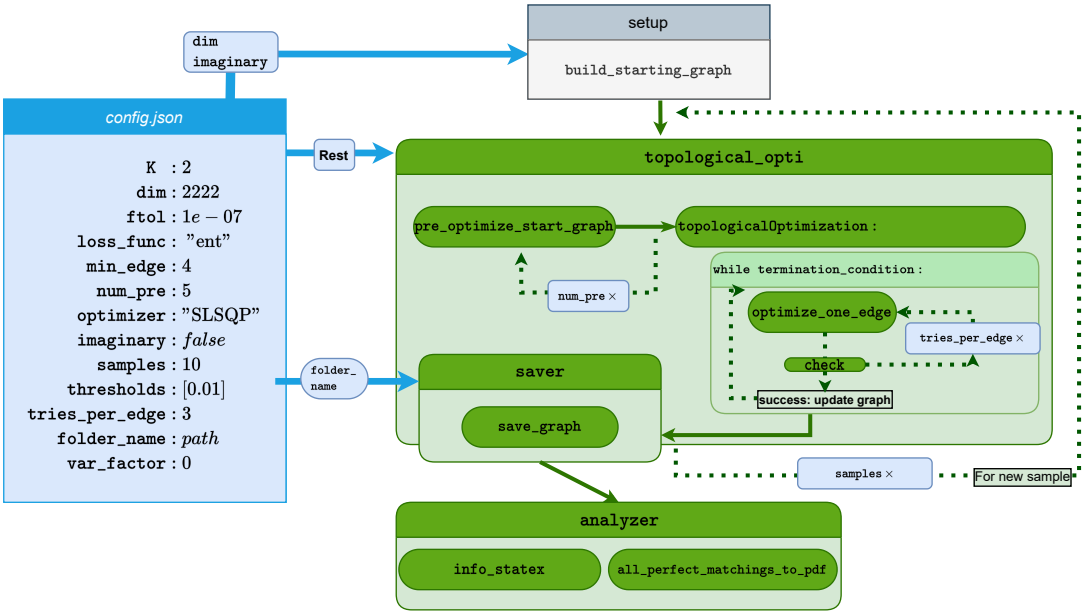

Figure 5 Schematic overview over the library THESEUS.

[2] https://github.com/artificial-scientist-lab/Theseus.git

3 Results

During the search for entangled states, we have limited ourselves mainly to the systems of qubits and qutrits given in Table 1. In the following we will specify all states with omitted normalization. For simplicity, we introduce the following notation. For a given state $|\Psi\rangle$ and a given bipartion B with the reduced density matrix ρ_{red} the normalized concurrence reads

$$C_n\left(|\Psi\rangle\right) = \frac{C\left(\Psi\right)}{\beta_{\text{max}}} = \frac{\sqrt{2 \cdot \left(1 - \operatorname{Tr} \rho_{\text{red}}^2\right)}}{\beta_{\text{max}}},$$

where β_{max} is the maximum value the entropy can have for that split. This means if a state is separable the result is zero and if the reduced density matrix is maximally mixed the result is equal one. We denote a state resulting from the optimization for n particles of dimension d with loss function L as follows

$$|\mathrm{Ent(n,d,k)}\rangle \quad \text{or} \quad |\mathrm{Ent(n,d,k)_c}\rangle \quad , \tag{3.1}$$

where the subscript c denotes the optimization with complex weights. For the graphs shown, the white diamonds symbolize that the corresponding edge weight is negative. All used `config files` can be found in the mentioned GitHub.

3.1 Four Qubits

For a system of four qubits, the optimization finds a variety of results. One example reads

$$|\mathrm{Ent}(4,2,2)\rangle = |1010\rangle + |1101\rangle - (|0011\rangle + |0100\rangle). \tag{3.2}$$

The state $|\mathrm{Ent}(4,2,2)\rangle$ is maximally entangled for all bipartitions except for $\{AC, BD\}$. When one optimizes for complex values and setting $\texttt{var\_fac} = 5$ one can obtain a state similar to the $|HS\rangle$ state

$$\begin{aligned}|\mathrm{Ent}(4,2,2)_c\rangle =& e^{0.02 \cdot i \cdot \pi} \cdot |0011\rangle + e^{-0.52 \cdot i \cdot \pi} \cdot |0101\rangle + e^{-0.91 \cdot i \cdot \pi} \cdot |0110\rangle + \\ & e^{0.47 \cdot i \cdot \pi} \cdot |1001\rangle + e^{\,0.73 \cdot i \cdot \pi} \cdot |1010\rangle + e^{0.88 \cdot i \cdot \pi} \cdot |1100\rangle\end{aligned}$$

That state is k=1 uniform but compared to $|\Psi_{2222}\rangle$ the entanglement is distributed over all bipartions meaning for the three bipartion with length two the normalized entropy reads 0.943 which is equivalent to the $|\mathrm{HS}\rangle$ state. The corresponding graphs are shown in 6.

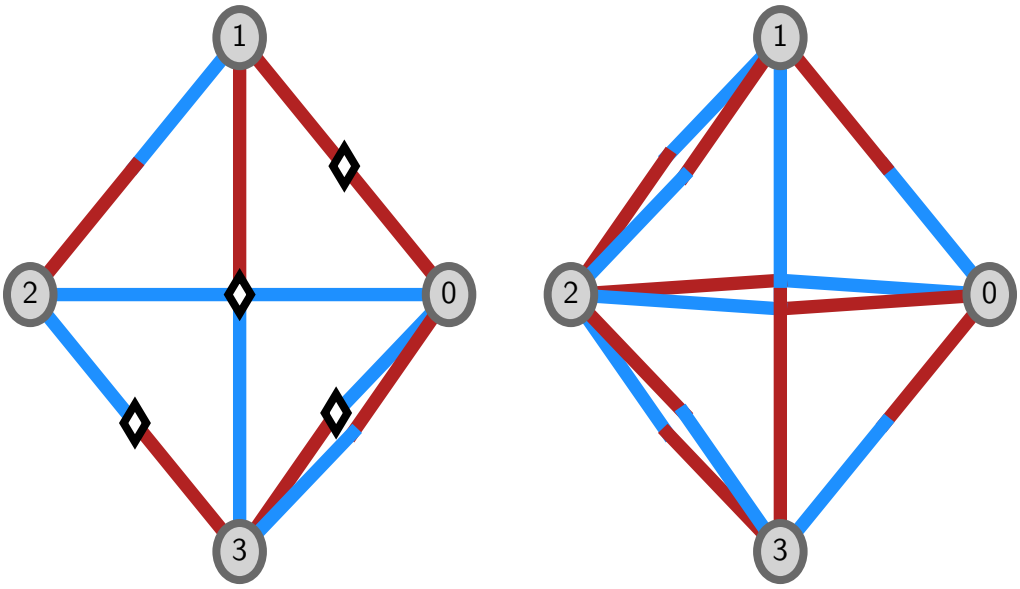

Figure 6 The left graph is for the state $|\mathrm{Ent}(4,2,2)\rangle$ having six edges and four PMs with all weights $\omega_i = \pm 1$. The right graph is for the state $|\mathrm{Ent}(4,2,2)_c\rangle$ having nine edges and six PMs with.

3.2 Five Qubits

Optimizing entanglement for five qubits one can find an experimental realization of a corresponding AME. Figure 7 shows the graph for the states

$$\begin{aligned}|\mathrm{Ent}(5,2,2)_1\rangle = &|00000\rangle + |01101\rangle + |01110\rangle + |10110\rangle + \\ &|11000\rangle + |11011\rangle - |00011\rangle - |10101\rangle \\ |\mathrm{Ent}(5,2,2)_2\rangle = &|01011\rangle + |01100\rangle + |10110\rangle + |11010\rangle - \\ &|00000\rangle - |00111\rangle - |10001\rangle - |11101\rangle\end{aligned}$$

Those states are equivalent with respect to LOCC (local operations and classical communication) to the states $|0_L\rangle$ and $|1_L\rangle$ respectively that were used for a quantum error correction code in Laflamme et al., 1996.

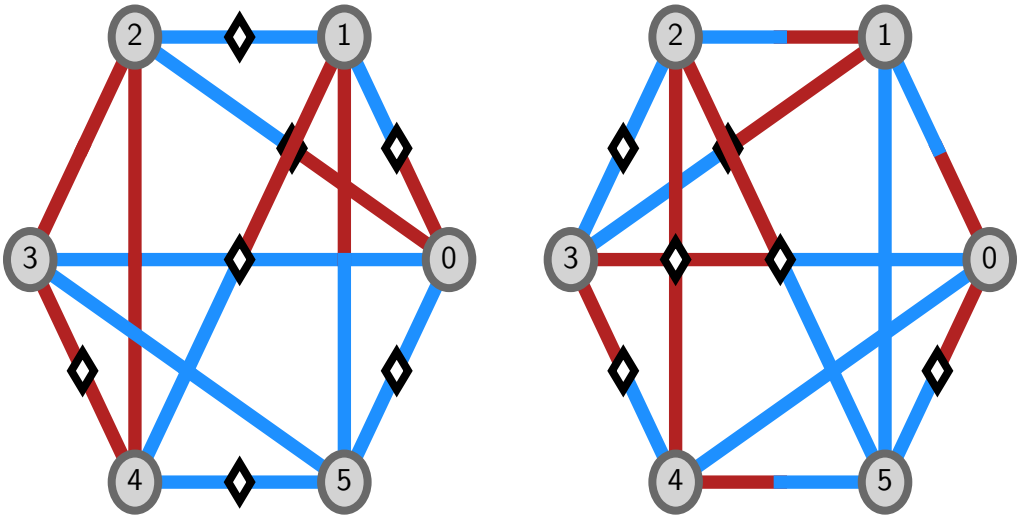

Figure 7 The left graph is for the state $|\mathrm{Ent}(5,2,2)_1\rangle$, the right one for $|\mathrm{Ent}(5,2,2)_2\rangle$. Both have 12 edges and eight PMs with all weights $\omega_i = \pm 1$.

3.3 Six Qubits

Optimizing for a system of six qubits with a loss function $\mathcal{L}_{k=2}$ for two uniform states we found the following state

$$\begin{aligned}|\mathrm{Ent}(6,2,2)\rangle = &|100011\rangle + |101110\rangle - (|000000\rangle + |001101\rangle + \\ &|010111\rangle + |011010\rangle + |110100\rangle + |111001\rangle)\end{aligned}$$

The graph is shown in Figure 8. It is k=2 uniform and from $\binom{6}{3} = 20$ possible three bipartions are 12 maximal mixed and for the remaining eight the normalized entropy reads 0.926. Interestingly, we also found a epsilon solution for the existing AME(6,2). One can write the weights $\omega_i(\epsilon)$ of the graph shown in Figure 8 in dependent of an $\epsilon > 0$ such that they have an analytic structure. Then the resulting state reads

$$\begin{aligned}|\mathrm{Ent}(6,2,3)\rangle = \epsilon\,(&|000010\rangle + |000100\rangle + |001001\rangle + |010101\rangle + \\ &|011000\rangle + |011110\rangle + |101010\rangle + |110000\rangle + \\ &|111011\rangle + |111101\rangle - |001111\rangle - |010011\rangle - \\ &|100001\rangle - |100111\rangle - |101100\rangle - |110110\rangle\,) \\ +\epsilon^2\,(&|000000\rangle + |000110\rangle + |010001\rangle + |010111\rangle + \\ &|110010\rangle + |110100\rangle + |111001\rangle + |111111\rangle\,)\,.\end{aligned}$$

All terms being linear in ϵ are needed for the known AME(6,2), while additional terms occur but are quadratic in ϵ. For $\epsilon \to 0$ only the contributions linear in ϵ are relevant. Because of the very interesting structure of this state all types of perfect machtchings are summarized in Figure 9.

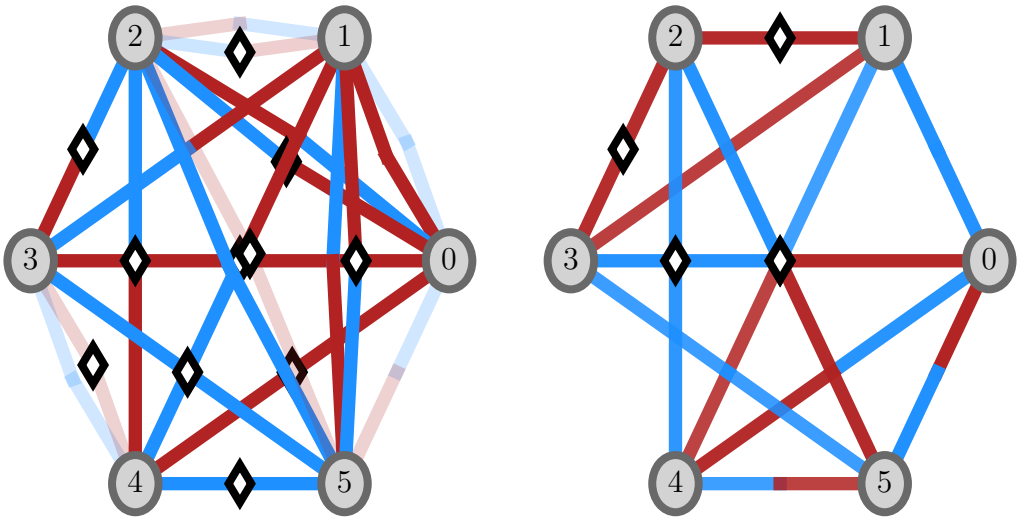

Figure 8 The graph on the left produces the $|\mathrm{Ent}(6,2,3)\rangle$. It has 21 edges and 41 PMs with all weights $\omega_i \in \{\pm\epsilon, \sqrt{2}, \pm 1, -\epsilon \cdot \sqrt{8}, \pm 1 \pm \epsilon\}$. The graph on the right produces the $|\mathrm{Ent}(6,2,2)\rangle$. It has 12 edges and eight PMs with all weights $\omega_i = \pm 1$.

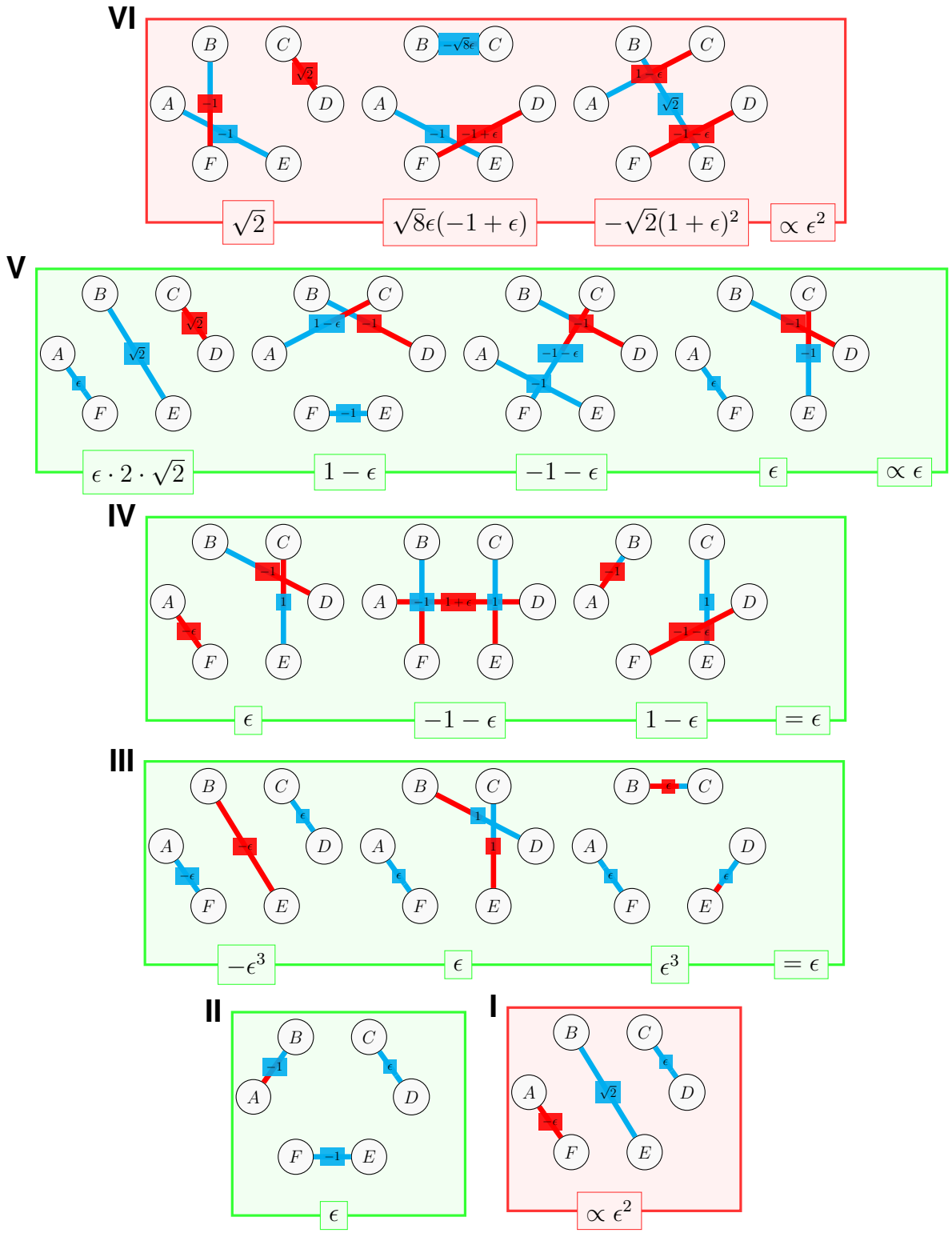

Figure 9 Figure shows the six different types of PMs occurring in the solution for the six Qubits Fake AME. Green background symbolizes that those are $\propto \epsilon$ and the red PMs are $\propto \epsilon$. The sum for each type stands at the right corner. Moreover there are also PMs of the same kind but with different sign.

3.4 Three and Four Qutrits

The three dimensional three-particle GHZ state is a k=1 uniform state and has been previously described as a graph (Krenn et al., 2021). All k=1 uniform states found here are equivalent to the GHZ state by local unitary operations. One example reads

$$|\mathrm{Ent}(3,3,1)\rangle = |010\rangle + |121\rangle + |202\rangle),$$

where one can find the corresponding graph in Figure 10. For the case of four qutrits we did not find a suitable graph for AME(4,3), for the existing AME(4,3) even with two or four with additional resources in the form of ancillary photons. Figure 10 shows a one uniform state with four qutrit being maximal entangled for all bipartions, except for $\{AB, CD\}$ it is separable. This can also be read directly from the graph, since there are no edges between the two nodes 0,1 and 2,3 and the two states can therefore be generated separately. The corresponding state reads

$$\begin{aligned}|\mathrm{Ent}(4,3,1)\rangle = &|0101\rangle + |0120\rangle + |1201\rangle + |1220\rangle + \\ &|2001\rangle + |2020\rangle - (|0112\rangle + |1212\rangle + |2012\rangle).\end{aligned}$$

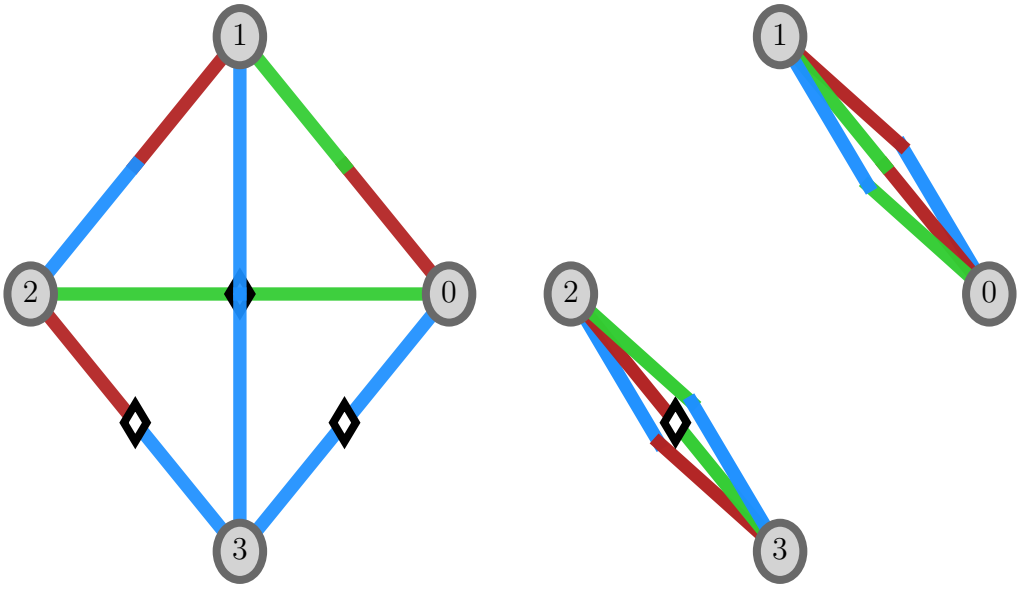

Figure 10 The graph on the left produces the state $|\mathrm{Ent}(3,3,1)\rangle$. It has six edges and three perfect matching with all weights $\omega_i = \pm 1$. The right graphs producing $|\mathrm{Ent}(4,3,1)\rangle$ has six edges and nine PMs whereby all weights read $\omega_i = \pm 1$.

3.5 Higher Dimensional Systems

For systems with higher dimensions or multiple particles, it turned out to be very difficult to find possible graphs corresponding to a k-uniform state except for $k = 1$. Neverthe-

less, we were able to find a nearly two uniform state for seven qubits, with 20 out of 21 bipartitions being maximally entangled, where for the one bipartion the normalized concurrence reads 0.63. This state reads

$$\begin{aligned}|\mathrm{Ent}(7,2,\mathrm{all})\rangle =&|0011110\rangle + |0101000\rangle + |0110111\rangle + \\ &|1001101\rangle + |1010010\rangle + |1100100\rangle \\ &- (|0000001\rangle + |1111011\rangle).\end{aligned}$$

The corresponding graph is shown in Figure 11. For eight qubits it was possible to find a two uniform state whereby 48 of 56 bipartitions of the bipartitions having length 3, were maximally entangled. This state reads

$$\begin{aligned}|\mathrm{Ent}(8,2,4)\rangle =&|00010000\rangle + |00010111\rangle + |01101011\rangle + \\ &|01101100\rangle + |01110001\rangle + |10100010\rangle + \\ &|10100101\rangle + |10111111\rangle + |11000100\rangle + \\ &|11011001\rangle - (|00001010\rangle + |00001101\rangle + \\ &|01110110\rangle + |10111000\rangle + |11000011\rangle + \\ &|11011110\rangle).\end{aligned}$$

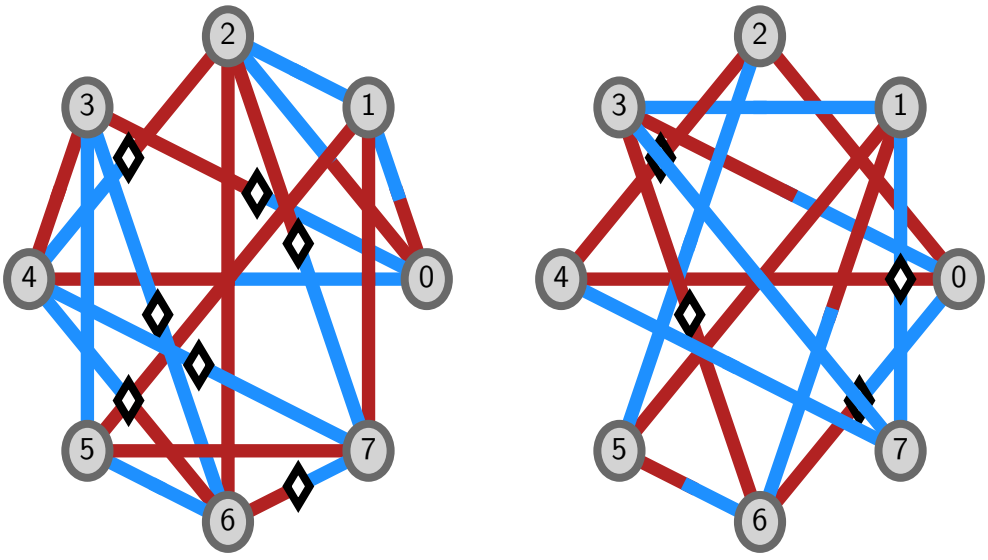

Figure 11 The right graph corresponds to $|\mathrm{Ent}(7,2,\mathrm{all})\rangle$ having 14 edges and eight PMs with all weights $\omega_i = \pm 1$. The left graphs producing $|\mathrm{Ent}(8,2,4)\rangle$ has 18 edges and 20 PMs whereby all weights read $\omega_i = \pm 1$.

3.6 Discussion and Outlook

The question posed at the beginning that how must a experimental setup look like to get the maximally entangled state according to a given entanglement measurement with a given set of experimental constraints, like amount of linear optic components producing N photons of dimensionality d_i, could be answered. To give an order of magnitude of the search space for five qubits, one can look at the possibilities on graphs with weights $\omega = \pm 1$, which is roughly $2.4 \cdot 10^{23}$. The fact that one finds an AME as result shows the efficiency of THESEUS. For higher systems, however, the search is more difficult. Here extensions would be conceivable which set up a random start graph constellation for larger systems to make the search easier. Also it would be interesting to investigate if there exists generalization or a pattern for the AMEs or k uniform graphs similar to the construction over orthogonal arrays (Li & Yan-Ling, 2019). For this purpose, AI could be used again, for example with an algorithm that transforms the graphs into a simple 3d structure in order to recognize structures more easily. Another interesting approach would be to build a database with properties of different graphs, e.g. adjacent matrix or its eigenvalues and also the entanglement measure of the resulting state. Afterwards, one could use clustering or neural networks to draw conclusions about patterns. This could allow an even deeper understanding of the graphs. Furthermore, it was impressively shown that the basic idea of using AI to advance scientific discoveries and to make them understandable for scientists is a sustainable approach. In other areas of research, too, it can be seen that the use of machine learning approaches can advance research. Be it as a diagnostic tool in medicine (Kaplan et al., 2021), as a control for fusion reactor (Seo et al., 2022), to search for alternative physics (Chen et al., 2022) or simply to understand humans better (Sun et al., 2022). So it remains exciting what discoveries we can expect from AI and what role we scientist will play in the future.

4 Acknowledgement

At this point I would like to thank all those who supported and motivated me during the preparation of this bachelor thesis.

First and foremost, I would like to thank Sören Arlt, who supervised my work and helped me with many answers to my questions and numerous suggestions. I would also like to thank Carlos Ruiz González for the numerous suggestions and discussions. Last but not least, I would like to thank Professor Krenn, who was often able to give me great thoughts and suggestions also beyond the bachelor thesis.

I would also like to thank my girlfriend Veronika Riedl, who supported me with a lot of patience and helpfulness and especially for making the great drawing at the beginning.

I would also like to thank Timon Petermann and Lisa Elsner for proofreading my bachelor thesis.

References

Aspect, A. (1999). Bell's inequality test: More ideal than ever. *Nature*, *398*, 189–190.

Bartholomew–Biggs, M. (2008). Sequential quadratic programming. *Nonlinear optimization with engineering applications* (pp. 1–14). Springer US. https://doi.org/10.1007/978-0-387-78723-7_19

Bennett, C. H., & Wiesner, S. J. (1992a). Communication via one- and two-particle operators on einstein-podolsky-rosen states. *Phys. Rev. Lett.*, *69*, 2881–2884. https://doi.org/10.1103/PhysRevLett.69.2881

Bennett, C. H., & Wiesner, S. J. (1992b). Communication via one- and two-particle operators on einstein-podolsky-rosen states. *Phys. Rev. Lett.*, *69*, 2881–2884. https://doi.org/10.1103/PhysRevLett.69.2881

Bhaskara, V. S., & Panigrahi, P. K. (2017). Generalized concurrence measure for faithful quantification of multiparticle pure state entanglement using lagrange's identity and wedge product. *Quantum Information Processing*, *16*(5). https://doi.org/10.1007/s11128-017-1568-0

Chen, B., Huang, K., Raghupathi, S., Chandratreya, I., Du, Q., & Lipson, H. (2022). Automated discovery of fundamental variables hidden in experimental data. *Nature Computational Science*, *2*, 433–442. https://doi.org/10.1038/s43588-022-00281-6

Einstein, A., Podolsky, B., & Rosen, N. (1935). Can quantum-mechanical description of physical reality be considered complete? *Phys. Rev.*, *47*, 777–780. https://doi.org/10.1103/PhysRev.47.777

Giustina, M., Versteegh, M. A., Wengerowsky, S., Handsteiner, J., Hochrainer, A., Phelan, K., Steinlechner, F., Kofler, J., Larsson, J.-Å., Abellán, C., Amaya, W., Pruneri, V., Mitchell, M. W., Beyer, J., Gerrits, T., Lita, A. E., Shalm, L. K., Nam, S. W., Scheidl, T., … Zeilinger, A. (2015). Significant-loophole-free test of bell's theorem with entangled photons. *Physical Review Letters*, *115*(25). https://doi.org/10.1103/physrevlett.115.250401

Gour, G., & Wallach, N. R. (2010). All maximally entangled four-qubit states. *Journal of Mathematical Physics*, *51*(11), 112201. https://doi.org/10.1063/1.3511477

Goyeneche, D., & Zyczkowski, K. (2014). Genuinely multipartite entangled states and orthogonal arrays. *Physical Review A*, *90*(2). https://doi.org/10.1103/physreva.90.022316

Goyeneche, D., & Życzkowski, K. (2014). Genuinely multipartite entangled states and orthogonal arrays. *Physical Review A*, *90*(2). https://doi.org/10.1103/physreva.90.022316

Greenberger, D. M., Horne, M. A., & Zeilinger, A. (2007). Going beyond bell's theorem. https://doi.org/10.48550/ARXIV.0712.0921

Guedes, E. B., de Assis, F. M., & Medeiros, R. A. C. (2016). Fundamentals of quantum information processing. *Quantum zero-error information theory* (pp. 7–26). Springer International Publishing. https://doi.org/10.1007/978-3-319-42794-2_2

Helwig, W. (2013). Absolutely maximally entangled qudit graph states. https://doi.org/10.48550/ARXIV.1306.2879

Higuchi, A., & Sudbery, A. (2000). How entangled can two couples get? *Physics Letters A*, *273*(4), 213–217. https://doi.org/10.1016/s0375-9601(00)00480-1

Hill, S. A., & Wootters, W. K. (1997). Entanglement of a pair of quantum bits. *Phys. Rev. Lett.*, *78*, 5022–5025. https://doi.org/10.1103/PhysRevLett.78.5022

Kaplan, A., Cao, H., FitzGerald, J. M., Iannotti, N., Yang, E., Kocks, J. W., Kostikas, K., Price, D., Reddel, H. K., Tsiligianni, I., Vogelmeier, C. F., Pfister, P., & Mastoridis, P. (2021). Artificial intelligence/machine learning in respiratory medicine and potential role in asthma and copd diagnosis. *The Journal of Allergy and Clinical Immunology: In Practice*, *9*(6), 2255–2261. https://doi.org/https://doi.org/10.1016/j.jaip.2021.02.014

Kiefer, C. (2015). Die arbeit von einstein, podolsky und rosen. In C. Kiefer (Ed.), *Albert einstein, boris podolsky, nathan rosen: Kann die quantenmechanische beschreibung der physikalischen realität als vollständig betrachtet werden?* (pp. 27–54). Springer Berlin Heidelberg. https://doi.org/10.1007/978-3-642-41999-7-2

Krenn, M., Kottmann, J. S., Tischler, N., & Aspuru-Guzik, A. (2021). Conceptual understanding through efficient automated design of quantum optical experiments. *Physical Review X*, *11*(3). https://doi.org/10.1103/physrevx.11.031044

Krenn, M., Malik, M., Fickler, R., Lapkiewicz, R., & Zeilinger, A. (2016). Automated search for new quantum experiments. *Physical Review Letters*, *116*(9). https://doi.org/10.1103/physrevlett.116.090405

Laflamme, Miquel, Paz, & Zurek. (1996). Perfect quantum error correcting code. *Physical review letters*, *77 1*, 198–201.

Li, M.-S., & Yan-Ling, W. (2019). K-uniform quantum states arising from orthogonal arrays. *Physical Review A*, *99*. https://doi.org/10.1103/PhysRevA.99.042332

Mattle, K., Weinfurter, H., Kwiat, P. G., & Zeilinger, A. (1996). Dense coding in experimental quantum communication. *Phys. Rev. Lett.*, *76*, 4656–4659. https://doi.org/10.1103/PhysRevLett.76.4656

Plbnio, M. B., & Virmani, S. (2007). An introduction to entanglement measures. *Quantum Info. Comput.*, *7*(1), 1–51.

Raissi, Z., Gogolin, C., Riera, A., & Acın, A. (2018). Optimal quantum error correcting codes from absolutely maximally entangled states. *Journal of Physics A: Mathematical and Theoretical*, *51*(7), 075301. https://doi.org/10.1088/1751-8121/aaa151

Rungta, P., Buek, V., Caves, C. M., Hillery, M., & Milburn, G. J. (2001). Universal state inversion and concurrence in arbitrary dimensions. *Physical Review A*, *64*(4). https://doi.org/10.1103/physreva.64.042315

Schumacher, B. (1995). Quantum coding. *Phys. Rev. A*, *51*, 2738–2747. https://doi.org/10.1103/PhysRevA.51.2738

Scott, A. J. (2004). Multipartite entanglement, quantum-error-correcting codes, and entangling power of quantum evolutions. *Physical Review A*, *69*(5). https://doi.org/10.1103/physreva.69.052330

Seo, J., Na, Y.-S., Kim, B., Lee, C., Park, M., Park, S., & Lee, Y. (2022). Development of an operation trajectory design algorithm for control of multiple 0d parameters using deep reinforcement learning in KSTAR. *Nuclear Fusion*, *62*(8), 086049. https://doi.org/10.1088/1741-4326/ac79be

Shi, F., Shen, Y., Chen, L., & Zhang, X. (2020). Constructions of k-uniform states from mixed orthogonal arrays. https://doi.org/10.48550/ARXIV.2006.04086

Shor, P. W. (1997). Polynomial-time algorithms for prime factorization and discrete logarithms on a quantum computer. *SIAM Journal on Computing*, *26*(5), 1484–1509. https://doi.org/10.1137/s0097539795293172

Sun, Z., Ke, Q., Rahmani, H., Bennamoun, M., Wang, G., & Liu, J. (2022). Human action recognition from various data modalities: A review. *IEEE Transactions on Pattern Analysis and Machine Intelligence*, 1–20. https://doi.org/10.1109/TPAMI.2022.3183112

Union, E. (2019). *The european quantum communication infrastructure (euroqci) initiative*. Retrieved August 12, 2022, from https://digital-strategy.ec.europa.eu/en/policies/european-quantum-communication-infrastructure-euroqci

Union, E. (2021). *Eu innovation moves one step closer to the world's first compact quantum computer*. Retrieved August 12, 2022, from https://digital-strategy.ec.europa.eu/en/news/eu-innovation-moves-one-step-closer-worlds-first-compact-quantum-computer

Wang, J., Sciarrino, F., Laing, A., & Thompson, M. G. (2019). Integrated photonic quantum technologies. *Nature Photonics*, *14*(5), 273–284. https://doi.org/10.1038/s41566-019-0532-1

Weihs, G., Jennewein, T., Simon, C., Weinfurter, H., & Zeilinger, A. (1998). Violation of bell's inequality under strict einstein locality conditions. *Phys. Rev. Lett.*, *81*, 5039–5043. https://doi.org/10.1103/PhysRevLett.81.5039

Zha, X., Yuan, C., & Zhang, Y. (2013). Generalized criterion for a maximally multi-qubit entangled state. *Laser Physics Letters*, *10*(4), 045201. https://doi.org/10.1088/1612-2011/10/4/045201

Declaration of Academic Integrity

I hereby declare that this thesis and the work presented in it is entirely my own. Where I have consulted the work of others, this is always clearly attributed. Where I have quoted from the work of others, the source is always given. I am aware that the thesis in digital form can be examined for the use of unauthorised aid and in order to determine whether the thesis as a whole or in parts may amount to plagiarism. I am aware that a false assurance fulfils the elements of fraud in accord with § 10 and § 13 ABM-PO/TechFak and will result in the consequences proclaimed there. This paper was not previously presented to another examination board and has not been published.

Erlangen, 5th November 2022

Jan Petermann